

**ADVANCING METHODS FOR DETERMINING THE SOURCE OF  
HEU USED IN A TERRORIST NUCLEAR WEAPON**

A Senior Scholars Thesis

by

ADRIENNE MARIE LAFLEUR

Submitted to the Office of Undergraduate Research  
Texas A&M University  
In partial fulfillment of the requirements for the designation as

UNDERGRADUATE RESEARCH SCHOLAR

April 2007

Major: Nuclear Engineering

**ADVANCING METHODS FOR DETERMINING THE SOURCE OF  
HEU USED IN A TERRORIST NUCLEAR WEAPON**

A Senior Scholars Thesis

by

ADRIENNE MARIE LAFLEUR

Submitted to the Office of Undergraduate Research  
Texas A&M University  
In partial fulfillment of the requirements for the designation as

UNDERGRADUATE RESEARCH SCHOLAR

Approved by:

Research Advisor:  
Associate Dean for Undergraduate Research:

William S. Charlton  
Robert C. Webb

April 2007

Major: Nuclear Engineering

## ABSTRACT

Advancing Methods for Determining the Source of HEU Used in Terrorist Nuclear  
Weapon (April 2007)

Adrienne M. LaFleur  
Department of Nuclear Engineering  
Texas A&M University

Research Advisor: Dr. William Charlton  
Department of Nuclear Engineering

An algorithm was developed that uses measured isotopic ratios from fission product residue following the detonation of a high-enriched uranium nuclear weapon to compute the original attributes of the material used in the device. The specific attributes assessed are the uranium isotopics (considering  $^{234}\text{U}$ ,  $^{235}\text{U}$ ,  $^{236}\text{U}$ , and  $^{238}\text{U}$ ) and the enrichment process used to create the material (e.g., gaseous diffusion, gas centrifuge, etc.). Using the original attributes of the weapon significantly increases the probability of identifying the perpetrator of the attack. In this study, research was conducted to perform sensitivity analysis of the calculated values, analyze alternate enrichment methods, determine the source (uranium mine) from which the feed material was taken and assess potential “spoofing” techniques. The purpose of this research was to verify that the analytical method developed would remain valid for a multitude of variations that could be used to disguise the origin of the nuclear material in the device. It is envisioned that this methodology could serve as a preprocessing step to a more computationally intensive and more accurate system in the event of a nuclear terrorist attack.

## ACKNOWLEDGMENTS

I would especially like to thank Dr. Charlton for all of his help and expertise during the completion of this thesis. Dr. Charlton contributed a great amount of his time to helping me with this work. I also appreciate the help provided by Diane Fischer and Mark Laughter from Oak Ridge National Laboratory and by Lee Cadwallader from Idaho National Laboratory.

This research was performed while on appointment as a U.S. Department of Homeland Security (DHS) Scholar under the DHS Scholarship and Fellowship Program, a program administered by the Oak Ridge Institute for Science and Education (ORISE) for DHS through an interagency agreement with the U.S Department of Energy (DOE). ORISE is managed by Oak Ridge Associated Universities under DOE contract number DE-AC05-00OR22750. All opinions expressed in this paper are the author's and do not necessarily reflect the policies and views of DHS, DOE, or ORISE.

## TABLE OF CONTENTS

	Page
ABSTRACT .....	iii
ACKNOWLEDGMENTS.....	iv
TABLE OF CONTENTS.....	v
LIST OF FIGURES .....	vii
LIST OF TABLES.....	viii
CHAPTER	
I INTRODUCTION.....	1
Scenario of interest.....	1
Attribution of an HEU nuclear weapon.....	3
Project overview .....	5
II METHODOLOGY .....	8
Forward model development .....	8
Inverse model development.....	10
III URANIUM SIGNATURES .....	14
Enrichment processes .....	14
Presence of <sup>236</sup> U .....	20
IV SENSITIVITY ANALYSIS.....	22
Sensitivity of initial guess for <sup>235</sup> U concentration.....	22
Sensitivity of error in calculated <sup>234</sup> U attribute.....	23
Sensitivity of error in calculated <sup>235</sup> U attribute.....	25
Sensitivity of error in calculated <sup>236</sup> U attribute.....	28
V <sup>234</sup> U ISOTOPICS IN MINES .....	30

VI	DISCUSSION AND CONCLUSION .....	33
	Discussion.....	33
	Conclusion.....	35
	REFERENCES .....	37
	APPENDIX A .....	39
	APPENDIX B.....	41
	CONTACT INFORMATION .....	45

## LIST OF FIGURES

FIGURE	Page
1 Assembly system for a gun-type weapon .....	2
2 Technical routes to a nuclear capability .....	4
3 ORIGEN2 calculation of $^{236}\text{U}/^{235}\text{U}$ isotopic ratio versus irradiation time .....	13
4 Centrifuge for uranium separation .....	15
5 A gaseous diffusion stage used for uranium enrichment.....	16
6 Uranium enrichment process based on electromagnetic isotope separation .....	17
7 Uranium enrichment process based on atomic vapor laser isotope separation....	18
8 Error in the calculated $^{234}\text{U}/^{238}\text{U}$ value as a function of error in the measured $^{232}\text{U}$ value and the $^{234}\text{U}(n, 3n)$ microscopic cross-section .....	25
9 Error in the calculated $^{235}\text{U}/^{238}\text{U}$ value as a function of error in the $^{235}\text{U}$ enrichment and the $^{235}\text{U}$ microscopic fission cross-section.....	27
10 Error in the calculated $^{236}\text{U}/^{238}\text{U}$ value as a function of errors in the $^{236}\text{U}$ and the $^{235}\text{U}$ microscopic absorption cross-sections.....	29
11 The $^{234}\text{U}/^{235}\text{U}$ atom ratio measured in all twelve samples.....	32
12 Expanded plot of the measured $^{234}\text{U}/^{235}\text{U}$ atom ratios excluding sample 8.....	32

## LIST OF TABLES

TABLE	Page
I Comparison of inverse model calculations to the exact values for gaseous centrifuge and gaseous diffusion enriched fuel with $^{236}\text{U}$ .....	19
II Comparison of inverse model calculations to the exact values for gaseous centrifuge and gaseous diffusion enriched fuel without $^{236}\text{U}$ .....	20
III Comparison of inverse model calculations to the exact values for gaseous diffusion enriched fuel with and without $^{236}\text{U}$ .....	21
IV Comparison of inverse model calculations to the exact values for gaseous centrifuge enriched fuel with and without $^{236}\text{U}$ .....	21
V Comparison of values calculated by the inverse model with various initial guesses for the $^{235}\text{U}$ concentration to the actual values.....	23
VI Variations in measured $^{234}\text{U}/^{235}\text{U}$ atom ratios from mines throughout the world.....	31



# CHAPTER I

## INTRODUCTION

### **Scenario of interest**

One of the most crucial issues to national security in the United States is the ability to safeguard our country against nuclear terrorism. If national security was breached and a terrorist nuclear device was detonated in the United States, how quickly could we assess the site to determine what type of device was detonated, how powerful the device was and where it came from? Nuclear threats are not widely understood by the general population; therefore, if a terrorist device was ever detonated in our country immediate results must be produced in order to prevent mass hysteria.

The three types of weapons that use nuclear material are radiological dispersal devices (RDD), nuclear weapons, and improvised nuclear devices (IND). This work is focused on the post-detonation attribution of a Highly Enriched Uranium (HEU) terrorist nuclear weapon. Terrorist devices may differ from military nuclear weapons mainly in the sophistication applied when constructed (e.g., type and grade of material used and quality of tamper/reflector). Terrorist nuclear weapons that use HEU are typically gun-type weapons. This type of weapon requires approximately 25 kg of weapons-grade

---

This thesis follows the style of *Nuclear Technology*.

HEU and is detonated when a propellant blows one sub critical mass into the other forming a single supercritical mass and initiating a nuclear chain reaction. Since a gun-type weapon is considerably less complicated than an implosion weapon and more reliable (generally, gun-type weapons are not tested), this is considered to be a likely scenario for a nuclear terrorist attack.<sup>1</sup> The assembly system for a gun-type weapon is illustrated in Figure 1.

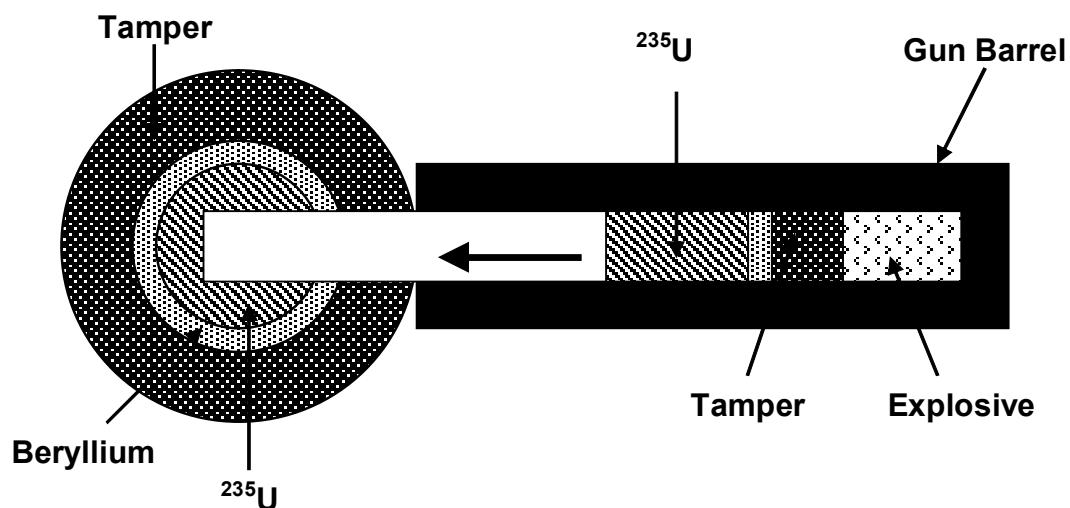


Fig. 1. Assembly system for a gun-type weapon.

The dispersal of fission products in the environment can vary greatly depending upon the altitude of weapon detonation. The most likely scenario for the detonation of a terrorist nuclear weapon would be on the ground. In this case, fission products would be dispersed on the ground within the blast radius of the weapon. To account for any non-

uniform fission of the HEU device, it is necessary to collect several samples along the diameter of the blast to determine if there are any significant variations in the concentration of fission products. The number of fissions in the device per unit mass may be calculated by using fission product measurements obtained from the ground samples. Two useful fission products to measure are  $^{89}\text{Sr}$  and  $^{95}\text{Zr}$  because they are characterized by low neutron absorption cross-sections and relatively long half-lives of 50.53 days and 64.02 days, respectively.<sup>2</sup> On the other hand, if a weapon was released from an aircraft and detonated at a high altitude, the fission products would be initially dispersed in the atmosphere before being deposited non-uniformly on ground. In this case, using measurements of noble gas fission products in the atmosphere, such as krypton and xenon, would provide the most accurate determination of the number of fissions in the device per unit mass.

### **Attribution of an HEU nuclear weapon**

The detonation of an HEU weapon would cause catastrophic damage and mass casualties. Due to the severity of such an attack, it is critical to be able to accurately identify the perpetrators responsible. A key deterrent to nuclear terrorism is the ability to compute the original material attributes of a weapon because it significantly increases the probability of correctly identifying perpetrators of the attack. The purpose of this research was to develop an algorithm that utilizes post-detonation measured isotopic ratios in order to determine the pre-detonation material attributes within reasonable accuracy. In general, post-nuclear event attribution of nuclear material occurs in several

stages where the first stage focuses on unambiguous process signatures such as uranium isotopic composition.<sup>3</sup> The process that nuclear material (both uranium and plutonium) undergoes in order to produce a nuclear weapon is illustrated in Fig. 2.

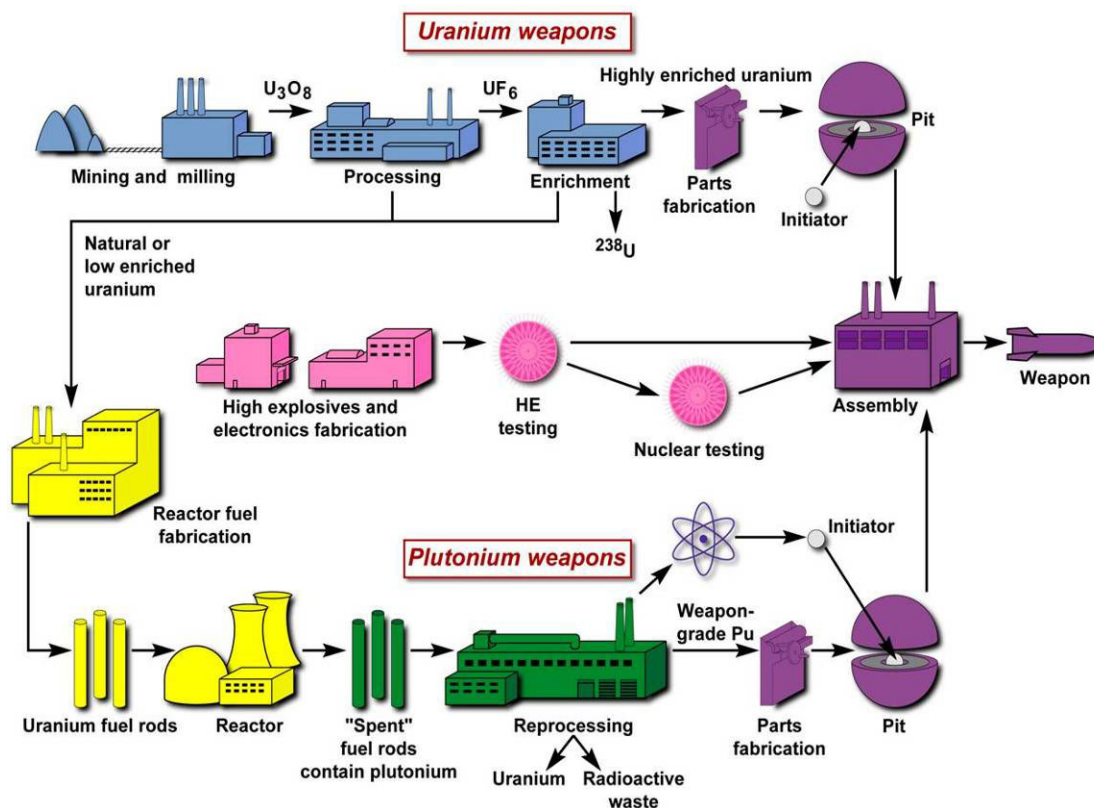


Fig. 2. Technical routes to a nuclear capability.

This study was focused only on the process used to produce an HEU nuclear weapon. The first step of this process consists of uranium mining and milling. The natural variation in the  $^{234}U$  concentration in uranium mines throughout the world provides a signature that is unique to this step of process.<sup>4</sup> This signature may be used to narrow

down the geographic location of the source (uranium mine) from which the feed material originated. The next step of the process analyzed in this study was uranium enrichment. Depending upon the method used to enrich uranium, increasing the  $^{235}\text{U}$  concentration also causes the  $^{234}\text{U}$  concentration to increase. Therefore the variation in the  $^{234}\text{U}$  concentration for various methods of enrichment provides a signature indicating what process was used to enrich the uranium. Once the enrichment process is known, it is also useful to determine whether or not  $^{236}\text{U}$  was present in the original material. Enriched uranium of U.S. or Russian origin contains a significantly higher abundance of  $^{236}\text{U}$  due to the re-enrichment of naval fuel which also provides a unique signature indicating where the uranium was enriched.

### **Project overview**

An algorithm was developed<sup>5</sup> that uses measured isotopic ratios from fission product residue following the detonation of a nuclear weapon to compute the original attributes of the nuclear material used in the weapon. The specific attributes assessed are the uranium isotopics (considering  $^{234}\text{U}$ ,  $^{235}\text{U}$ ,  $^{236}\text{U}$ , and  $^{238}\text{U}$ ) and the type of enrichment process used to create the material (e.g., gaseous diffusion, gas centrifuge, etc.). Before the methodology developed can be implemented, environmental measurements must be obtained from weapon debris to determine the isotopic composition of the post-detonation fission product residue and uranium source. Several methods may be used to perform these measurements. Preliminary measurements of the post-detonation fission product residue will most likely be performed using gamma spectroscopy because it is

non-destructive. In order to ensure accurate measurements using gamma spectroscopy, environmental samples will usually be counted on a High purity germanium (HPGe) detector for one to two days. Then, measurements of both the uranium and fission product isotopes will be performed using mass spectroscopy. This is the most accurate method for measuring ratios of isotopes from environmental samples.<sup>6</sup> The ability to measure both fission product ratios and uranium isotopic ratios to a high accuracy is necessary to ensure validity of the values calculated in the algorithm. Isotopic ratios of uranium relative to  $^{238}\text{U}$  can be measured using thermal ionization mass spectroscopy (TIMS) with a sensitivity of better than  $1.2 \times 10^{-10}$ .<sup>7</sup>

The approach to developing this algorithm consisted of two main parts: a forward model and an inverse model. The forward model consisted of simulations to predict post-detonation isotopics given the original isotopics of the material and the number of fissions (or yield) of the device. The inverse model calculated pre-detonation isotopics using analytical inversions of the buildup and decay equations (all first-order ordinary differential equations) and post-detonation isotopic measurements. The algorithm used was purely analytical, derived directly from burnup and radioactive decay equations. Thus, this methodology provided solutions with essentially no computational time required. In this study, further research was conducted to perform sensitivity analysis of the calculated values, analyze alternate enrichment methods, determine the source (uranium mine) from which the feed material was taken, and assess potential “spoofing” techniques.

Given a measurement of the post-detonation isotopes from fission product residue, the interest in this work was to attempt to determine the following characteristics (in this order of importance): (1) pre-detonation  $^{235}\text{U}$  enrichment, (2) pre-detonation  $^{234}\text{U}/^{238}\text{U}$  isotopic ratio, (3) pre-detonation  $^{236}\text{U}/^{238}\text{U}$  isotopic ratio, (4) enrichment method used to produce material, (5) pre-enrichment  $^{234}\text{U}/^{238}\text{U}$  isotopic ratio, (6) pre-enrichment  $^{236}\text{U}/^{238}\text{U}$  isotopic ratio, and (7) source (mine or otherwise) from which feed uranium was taken. It was acknowledged immediately that steps (1)-(3) would have a likely chance of success and the steps (4)-(7) would be significantly more difficult.

## CHAPTER II

### METHODOLOGY

#### **Forward model development**

The forward model consisted of simulations to predict post-detonation isotopics given the original isotopics of the material and the number of fissions (or yield) of the device. These simulations were performed using the ORIGEN2 computer code.<sup>8</sup> ORIGEN2 calculates the buildup and depletion of isotopics from irradiation and decay. The code possesses a large set of libraries (each library corresponds to a specific type of reactor) with cross-section, decay, and fission product yield data. ORIGEN2 uses the matrix exponential method to solve a large system of coupled, linear, first -order ordinary differential equations. While not a weapons burn code, ORIGEN contains sufficient capability to allow for analysis of the feasibility of the method developed here. In order to perform the ORIGEN2 calculations, a basic model of the ORIGEN2 code was created for an HEU weapon without <sup>236</sup>U present in the original fuel (see Appendix A).

Four different uranium signatures from gaseous centrifuge and gaseous diffusion enriched uranium, both with and without <sup>236</sup>U present in the original material, were simulated. The uranium was enriched to 95 a/o <sup>235</sup>U. The <sup>234</sup>U enrichment for gaseous centrifuge was calculated using the following equation:



$$\left(\frac{N^{234}}{N^{238}}\right)_0 = 0.007731 \left(\frac{N^{235}}{N^{238}}\right)_0^{1.0837} \left(\frac{M^{238}}{M^{235}}\right)^{1.0837} \quad (2.1)^*$$

where  $M^{238}$  is the atomic mass of  $^{238}\text{U}$  and  $M^{235}$  is the atomic mass of  $^{235}\text{U}$ . The following equation was used to calculate the  $^{234}\text{U}$  enrichment for gaseous diffusion:

$$\left(\frac{N^{234}}{N^{238}}\right)_0 = 0.008 \left(\frac{N^{235}}{N^{238}}\right)_0 \left(\frac{M^{238}}{M^{235}}\right) \quad (2.2)^*$$

Natural uranium contains essentially no  $^{236}\text{U}$  (though small quantities are found in natural material due to the activation of  $^{235}\text{U}$  from neutron background); however, enriched uranium of U.S. or Russian origin includes a significantly higher abundance of  $^{236}\text{U}$  due to the re-enrichment of naval fuel. The following equation represents the  $^{236}\text{U}$  enrichment in U.S. origin fuel:

$$\left(\frac{N^{236}}{N^{238}}\right)_0 = 0.0046 \left(\frac{N^{235}}{N^{238}}\right)_0 \left(\frac{M^{238}}{M^{235}}\right) \quad (2.3)^*$$

Then, the burnup of the initial material in the weapon given a 20 kT yield was simulated using ORIGEN2. Generally, a 2 kT yield is associated with terrorist weapons; however, this value was not used because only 2% of the original material fissions. The task of

---

\* These equations were taken from TransWare Enterprises Inc., "TransFX Computer Software Manuals," July 2001.

determining the original material used in the weapon becomes much simpler for low yields because there is only a slight difference between the pre-detonation composition and the post-detonation composition of the weapon. The resultant isotopes produced from this burnup were then decayed for 1.0 day (assumes that it will take approximately 1 day or more to acquire measurements from the post-detonation fission product residue). Assuming that the weapon was detonated on the ground or at a relatively low altitude,  $^{89}\text{Sr}$  and  $^{95}\text{Zr}$  (characterized by long half-lives, low absorption cross-sections, and the ability to be measured in the environment) were the two fission products used to calculate the total number of fission from the device in the inverse model.

### **Inverse model development**

The inverse model equations are all expressed in terms of atom ratios relative to  $^{238}\text{U}$  (the  $^{238}\text{U}$  concentration in the device is roughly constant during irradiation). The inverse model uses an iterative procedure where the pre-detonation  $^{235}\text{U}/^{238}\text{U}$  ratio is set to an initial guess input by the user. The pre-detonation  $^{234}\text{U}/^{238}\text{U}$  and  $^{236}\text{U}/^{238}\text{U}$  (if applicable) ratios were calculated using Eqs. (1)-(3) and then combined with the initial guess for  $^{235}\text{U}/^{238}\text{U}$  in order to calculate the  $^{235}\text{U}$  enrichment of the original material using:

$$e_0^i = \frac{\left(\frac{N^{235}}{N^{238}}\right)_0^{i-1}}{\left(\frac{N^{234}}{N^{238}}\right)_0^{i-1} + \left(\frac{N^{235}}{N^{238}}\right)_0^{i-1} + \left(\frac{N^{236}}{N^{238}}\right)_0^{i-1} + 1} \quad (2.4)$$

where  $e_0^i$  is the pre-detonation enrichment for step  $i$  and  $\left(\frac{N^x}{N^{238}}\right)_0^i$  is the pre-detonation atom ratio of isotope  $x$  to  $^{238}\text{U}$  from step  $i-1$  (or from the initial guess for the first step).

The number of fissions in the device per unit mass was calculated using the measurement of two fission products:  $^{95}\text{Zr}$  and  $^{89}\text{Sr}$ . A single fission product could have been used but by using two fission products, iteration between the two yielded a better prediction of the number of fissions. The following equation was used to calculate the number of fissions per unit mass in the device:

$$F_T^i = \left(\frac{N^{89}}{N^{238}}\right)_T \frac{N_A E_R}{M^{238} Y^{89}} e_0^i \left(\frac{N^{238}}{N^{235}}\right)_0^{i-1} \quad (2.5)$$

where  $F_T^i$  is the number of fissions in the device following irradiation (i.e., at time  $T$ ) per unit mass for step  $i$ ,  $\left(\frac{N^{89}}{N^{238}}\right)_T$  is the measured  $^{89}\text{Sr}/^{238}\text{U}$  atom ratio post-detonation (i.e., at time  $T$ ),  $N_A$  is Avogadro's number,  $E_R$  is the recoverable energy per fission, and  $Y^{89}$  is the cumulative fission product yield for  $^{89}\text{Sr}$ . In using Eq. (5) we assumed that the fission product yields and recoverable energy per fission from  $^{235}\text{U}$  was adequate (i.e., this assumes that all fissions were from  $^{235}\text{U}$ ).

An updated  $^{234}\text{U}/^{238}\text{U}$  value was then calculated using measurements of  $^{232}\text{U}/^{238}\text{U}$  in the residue and the following equation:

$$\left(\frac{N^{234}}{N^{238}}\right)_0^i = \left(\frac{N^{232}}{N^{238}}\right)_T \frac{\sigma_f^{235} E_R}{\sigma_{3n}^{234} F_T^i} \frac{N_A}{M^{235}} e_0^i \quad (2.6)$$

where  $\sigma_f^{235}$  is the one-group microscopic fission cross section for  $^{235}\text{U}$  and  $\sigma_{n,3n}^{234}$  is the one-group microscopic (n,3n) cross section for  $^{234}\text{U}$ . This equation assumes that no  $^{232}\text{U}$  existed in the original material and the measured  $^{232}\text{U}$  concentration was produced only from the  $^{234}\text{U}(n,3n)^{232}\text{U}$  reaction.

An updated  $^{235}\text{U}/^{238}\text{U}$  value was then calculated using measurements of  $^{235}\text{U}/^{238}\text{U}$  in the residue and the following equation:

$$\left(\frac{N^{235}}{N^{238}}\right)_0^i = \left(\frac{N^{235}}{N^{238}}\right)_T + \left(\frac{N^{235}}{N^{238}}\right)_0^{i-1} \frac{\sigma_a^{235} F_T^i}{\sigma_f^{235} E_R} \frac{M^{235}}{N_A} e_0^i \quad (2.7)$$

where  $\sigma_a^{235}$  is the one-group microscopic absorption cross section for  $^{235}\text{U}$ . This assumes that the change in  $^{235}\text{U}$  is equal to its loss rate from absorption.

Then, an updated  $^{236}\text{U}/^{238}\text{U}$  value was then calculated using measurements of  $^{236}\text{U}/^{238}\text{U}$  in the residue and the following equation:

$$\left(\frac{N^{236}}{N^{238}}\right)_0^i = \left(\frac{N^{236}}{N^{238}}\right)_T - \left(\frac{N^{235}}{N^{238}}\right)_0^i \frac{M^{235} F_T^i}{N_A e_0^i E_R} \left\{ \frac{\sigma_a^{235}}{\sigma_f^{235}} - 1 - \frac{\sigma_a^{236}}{2\sigma_f^{235}} \left[ \left(\frac{N^{236}}{N^{235}}\right)_0^{i-1} + \left(\frac{N^{236}}{N^{235}}\right)_T \right] \right\} \quad (2.8)$$

This equation assumes that the change in  $^{236}\text{U}$  is equal to its production rate from radiative capture in  $^{235}\text{U}$  minus the loss rate from the absorption of  $^{236}\text{U}$ . Equation (2.8) was obtained by assuming that the ratio of  $^{236}\text{U}/^{235}\text{U}$  as a function of irradiation time was linear and therefore was easily integrated. Verification of this assumption is illustrated in

Fig. 3 which depicts the ORIGEN2 calculated  $^{236}\text{U}/^{235}\text{U}$  isotopic ratio as a function of irradiation time. A linear trend line was used to fit to the data points.

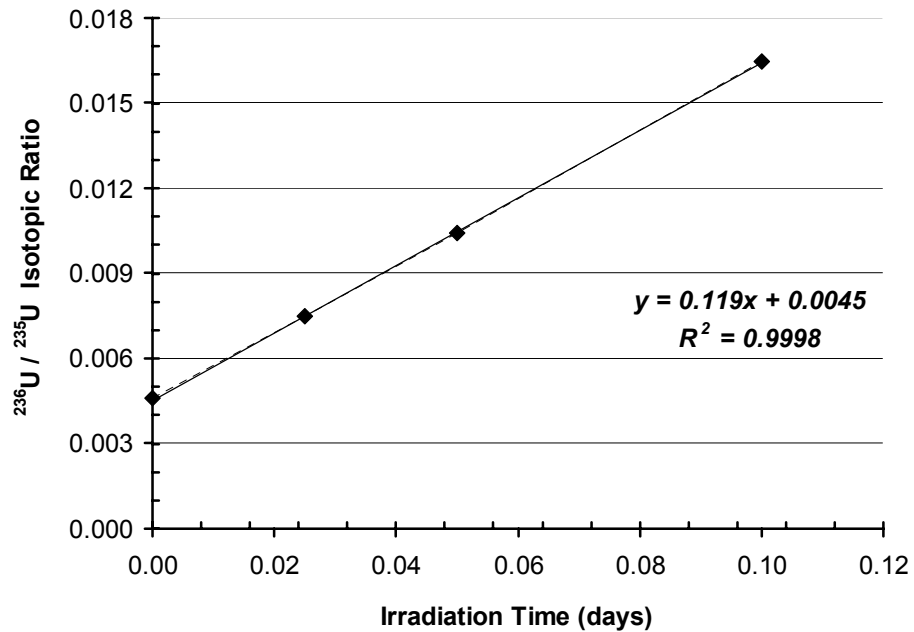


Fig 3. ORIGEN2 calculation of  $^{236}\text{U}/^{235}\text{U}$  isotopic ratio versus irradiation time.

A new value for the  $^{235}\text{U}$  enrichment was then calculated using Eq. (2.4). Equations (2.4) - (2.8) were repeated iteratively until the pre-detonation  $^{235}\text{U}/^{238}\text{U}$  ratio converged to a value within a specified tolerance.

## CHAPTER III

### URANIUM SIGNATURES

#### **Enrichment processes**

Weapons-grade HEU is typically enriched to 90 a/o  $^{235}\text{U}$  or greater. The method of enrichment provides a useful signature that may indicate where the uranium was enriched. Methods used to enrich uranium include: gaseous centrifuge, gaseous diffusion, electromagnetic isotope separation, and atomic vapor laser isotope separation.<sup>1</sup> The two most common enrichment processes used throughout the world are gaseous centrifuge and gaseous diffusion both of which separate the uranium isotopes in a gaseous compound called uranium hexafluoride.

#### *Gaseous Centrifuge*

In the gaseous centrifuge process, a rotor that is powered by an electric motor spins at high speeds in vacuum. The gas form of  $\text{UF}_6$  is introduced into the middle of the rotor and the resulting centrifugal force concentrates the heavier  $^{238}\text{UF}_6$  molecules towards the center while the lighter  $^{235}\text{UF}_6$  molecules are concentrated toward the axis of the rotor.<sup>9</sup> A slow axial countercurrent flow of gas increases the separation of these two isotopes by producing a small cascade within the centrifuge which concentrates the enriched gas at one end and depleted gas at the other. The separation capacity of one centrifuge is increased by increasing the length of the rotor and the rotor wall speed. An example of a centrifuge is illustrated in Fig. 4.

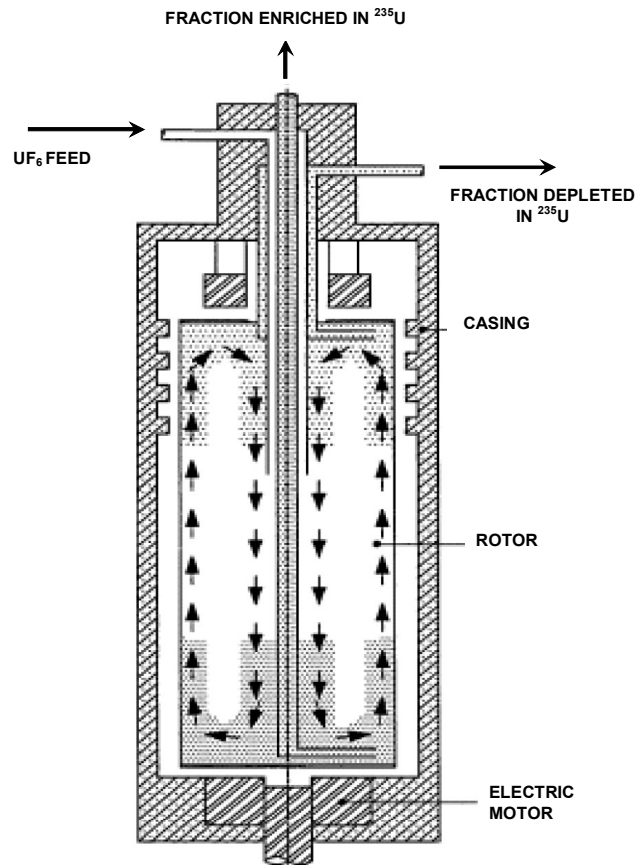


Fig. 4. Centrifuge for uranium separation.<sup>10</sup>

### *Gaseous Diffusion*

The gaseous diffusion process utilizes molecular effusion through small porous walls to separate the heavier  $^{238}\text{UF}_6$  molecules from the lighter  $^{235}\text{UF}_6$  molecules. The lower mass of the  $^{235}\text{UF}_6$  molecule causes it to move at a slightly higher velocity than the  $^{238}\text{UF}_6$  molecule which increases its probability of effusing through the walls. The difference in the velocity of a  $^{235}\text{UF}_6$  molecule versus a  $^{238}\text{UF}_6$  molecule is extremely small (approximately 0.4%) which causes the separation achieved by one gaseous diffusion to

be extremely small.<sup>9</sup> Therefore, numerous stages are required to produce LEU assays and over 4000 stages are required to produce HEU assays. A gaseous diffusion stage is illustrated in Fig. 5.

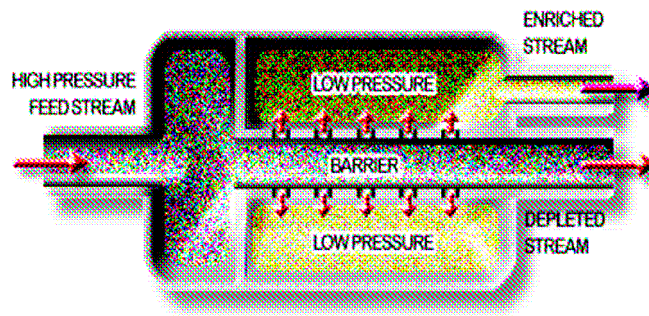


Fig. 5. A gaseous diffusion stage used for uranium enrichment.<sup>10</sup>

### *Electromagnetic Isotope Separation (EMIS)*

In the EMIS process,  $U^+$  ions are generated in an enclosed vacuum located in a magnetic field. An electrical potential is used to accelerate the ionized atoms which follow a circular trajectory in the plane perpendicular to the magnetic field. The radius of curvature of an ion's trajectory depends on the strength of the magnetic field and the mass of the ion, its electrical charge, and the speed of the ion. The lighter  $^{235}U$  ions are more easily deflected by the magnetic field and therefore have a smaller radius of curvature than the  $^{238}U$  ions, as illustrated in Fig. 6.<sup>1</sup> To put this in perspective, in an EMIS separator with a beam diameter of 4 feet the difference between the beam diameters for  $^{235}U$  and  $^{238}U$  is about 0.3 inches.



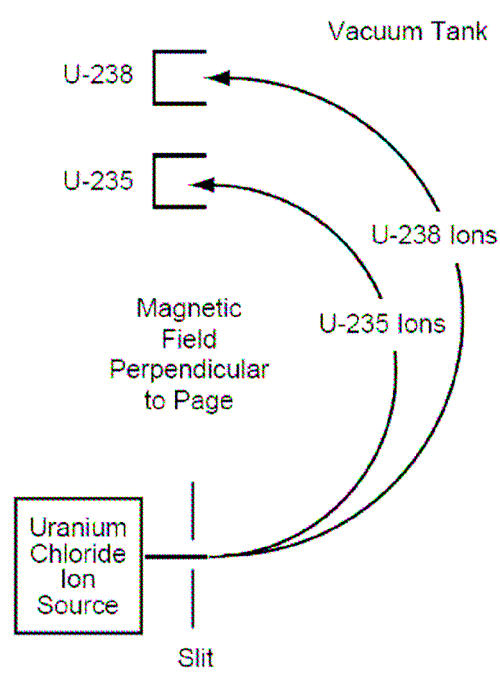


Fig. 6. Uranium enrichment process based on electromagnetic isotope separation.<sup>11</sup>

#### *Atomic Vapor Laser Isotope Separation (AVLIS)*

The AVLIS process for uranium enrichment is based on the principle that  $^{235}\text{U}$  atoms and  $^{238}\text{U}$  atoms have slightly different excited energy states and therefore absorb light at different frequencies. The lasers used in AVLIS are tuned to a precise frequency so that only the  $^{235}\text{U}$  atoms absorb the light. The AVLIS system is operated in vacuum and the uranium is heated to a molten state which occurs at temperatures above  $2000^{\circ}\text{C}$  (which is significantly greater than the melting temperature for metallic uranium of  $1130^{\circ}\text{C}$ ).

Uranium becomes vaporized at this molten state forming an atomic vapor stream which flows through the collector plates, where it is illuminated by a precisely tuned laser light

so only  $^{235}\text{U}$  atoms absorb the light. In order for a  $^{235}\text{U}$  atom to absorb enough energy to eject an electron and become a positively charged atom, three different lasers are used each tuned to precise frequency associated with a particular color in the ultraviolet spectrum. The ionized  $^{235}\text{U}$  atom is then deflected an electromagnetic field into the collector while the neutral  $^{238}\text{U}$  atom passes through to the tails collector (see Fig. 7).<sup>1</sup>

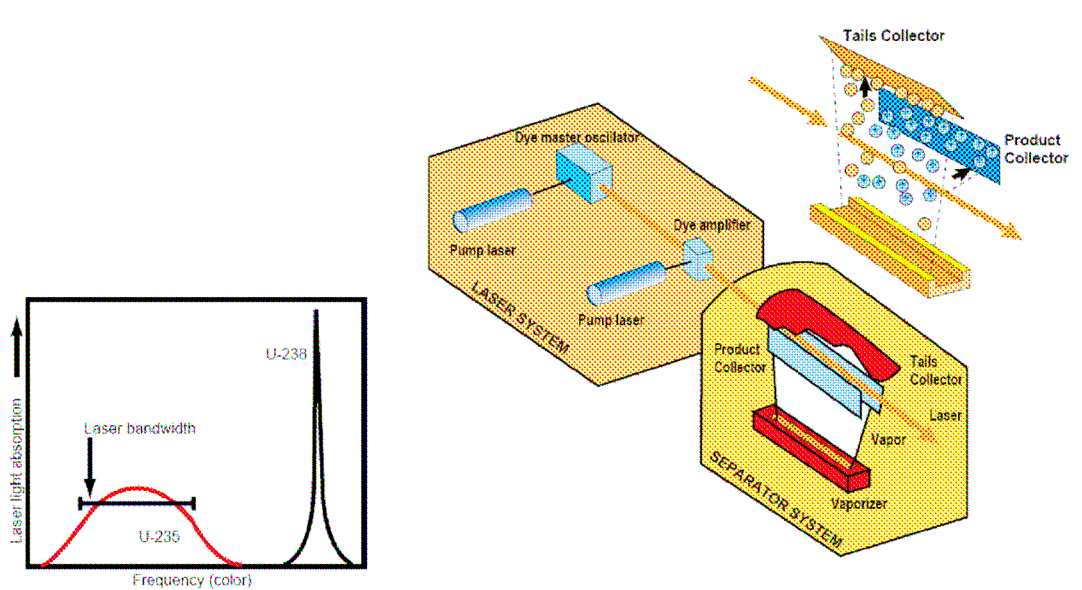


Fig. 7. Uranium enrichment process based on atomic vapor laser isotope separation.<sup>12</sup>

In this study, the algorithm developed analyzed only gaseous centrifuge and gaseous diffusion enrichment methods. These methods are hard to distinguish because they both rely on the differences in mass between  $^{235}\text{U}$  containing molecules and  $^{238}\text{U}$  containing molecules, though they are based on different physical processes. This results in small separation factors for both gaseous centrifuge and gaseous diffusion enrichment

methods, equal to 1.162 and 1.00429, respectively.<sup>13</sup> It is expected that distinguishing most other methods (such as AVLIS or EMIS) would be much simpler. For instance, the AVLIS uses precisely tuned lasers to enrich uranium resulting in a separation factor that is nearly infinite which yields almost no  $^{234}\text{U}$  in the enriched product.

In order to determine valid signatures indicating the method of enrichment, the values calculated in the inverse model for pre-detonation  $^{234}\text{U}$  concentrations were compared. For 95 a/o  $^{235}\text{U}$  centrifuge enriched fuel, the calculated  $^{234}\text{U}/^{238}\text{U}$  ratio was approximately 5.0 times greater than the calculated  $^{234}\text{U}/^{238}\text{U}$  ratio for 95 a/o  $^{235}\text{U}$  diffusion enriched fuel. These significant variations in  $^{234}\text{U}$  are presented in Table 1 and were used as signatures indicating the enrichment process used.

TABLE I.

Comparison of inverse model calculations to the exact values for gaseous centrifuge and gaseous diffusion enriched fuel with  $^{236}\text{U}$ .

<b>Enrichment Process</b>	<b>Atomic Ratio</b>	<b>Pre-Detonation Value (T = 0 days)</b>	<b>Inverse Model (T = 0 days)</b>	<b>Percent Error</b>
Centrifuge (with $^{236}\text{U}$ )	$\text{N}^{235}/\text{N}^{238}$	42.4	$43.1 \pm 0.411$	1.61%
	$\text{N}^{234}/\text{N}^{238}$	1.04	$1.06 \pm 0.015$	1.66%
	$\text{N}^{236}/\text{N}^{238}$	0.195	$0.204 \pm 0.011$	4.58%
Diffusion (with $^{236}\text{U}$ )	$\text{N}^{235}/\text{N}^{238}$	25.0	$25.4 \pm 0.254$	1.58%
	$\text{N}^{234}/\text{N}^{238}$	0.200	$0.204 \pm 0.003$	2.20%
	$\text{N}^{236}/\text{N}^{238}$	0.115	$0.121 \pm 0.007$	5.57%

TABLE II.

Comparison of inverse model calculations to the exact values for gaseous centrifuge and gaseous diffusion enriched fuel without  $^{236}\text{U}$ .

Enrichment Process	Atomic Ratio	Pre-Detonation Value (T = 0 days)	Inverse Model (T = 0 days)	Percent Error
Centrifuge (no $^{236}\text{U}$ )	$\text{N}^{235}/\text{N}^{238}$	35.5	$36.1 \pm 0.361$	1.62%
	$\text{N}^{234}/\text{N}^{238}$	0.869	$0.883 \pm 0.013$	1.69%
	$\text{N}^{236}/\text{N}^{238}$	0.0	$0.005 \pm 0.008$	-
Diffusion (no $^{236}\text{U}$ )	$\text{N}^{235}/\text{N}^{238}$	22.4	$22.6 \pm 0.225$	0.66%
	$\text{N}^{234}/\text{N}^{238}$	0.179	$0.182 \pm 0.005$	1.31%
	$\text{N}^{236}/\text{N}^{238}$	0.0	$0.027 \pm 0.003$	-

### Presence of $^{236}\text{U}$

After the enrichment process has been determined, whether or not  $^{236}\text{U}$  existed in original weapons material must be established. The values computed in the inverse model for gaseous diffusion and gaseous centrifuge enriched uranium, both with and without  $^{236}\text{U}$  present in the original material, are presented in Tables III and IV, respectively. For diffusion enriched fuel (with  $^{236}\text{U}$ ), the  $^{236}\text{U}$  value from the inverse model was approximately 4.5 times greater than the  $^{236}\text{U}$  value for diffusion enriched fuel (without  $^{236}\text{U}$ ).

TABLE III.

Comparison of inverse model calculations to the exact values for gaseous diffusion enriched fuel with and without  $^{236}\text{U}$ .

<b>Enrichment Process</b>	<b>Atomic Ratio</b>	<b>Pre-Detonation Value (T = 0 days)</b>	<b>Inverse Model (T = 0 days)</b>	<b>Percent Error</b>
Diffusion (with $^{236}\text{U}$ )	$\text{N}^{235}/\text{N}^{238}$	25.0	$25.4 \pm 0.254$	1.58%
	$\text{N}^{234}/\text{N}^{238}$	0.200	$0.204 \pm 0.003$	2.20%
	$\text{N}^{236}/\text{N}^{238}$	0.115	$0.121 \pm 0.007$	5.57%
Diffusion (no $^{236}\text{U}$ )	$\text{N}^{235}/\text{N}^{238}$	22.4	$22.6 \pm 0.225$	0.66%
	$\text{N}^{234}/\text{N}^{238}$	0.179	$0.182 \pm 0.005$	1.31%
	$\text{N}^{236}/\text{N}^{238}$	0.0	$0.027 \pm 0.003$	-

TABLE IV.

Comparison of inverse model calculations to the exact values for gaseous centrifuge enriched fuel with and without  $^{236}\text{U}$ .

<b>Enrichment Process</b>	<b>Atomic Ratio</b>	<b>Pre-Detonation Value (T = 0 days)</b>	<b>Inverse Model (T = 0 days)</b>	<b>Percent Error</b>
Centrifuge (with $^{236}\text{U}$ )	$\text{N}^{235}/\text{N}^{238}$	42.4	$43.1 \pm 0.411$	1.61%
	$\text{N}^{234}/\text{N}^{238}$	1.04	$1.06 \pm 0.015$	1.66%
	$\text{N}^{236}/\text{N}^{238}$	0.195	$0.204 \pm 0.011$	4.58%
Centrifuge (no $^{236}\text{U}$ )	$\text{N}^{235}/\text{N}^{238}$	35.5	$36.1 \pm 0.361$	1.62%
	$\text{N}^{234}/\text{N}^{238}$	0.869	$0.883 \pm 0.013$	1.69%
	$\text{N}^{236}/\text{N}^{238}$	0.0	$0.005 \pm 0.008$	-

## CHAPTER IV

### SENSITIVITY ANALYSIS

The methodology developed was tested for a 20 kT detonation of a 95 a/o  $^{235}\text{U}$  enriched HEU device. The “measured values” were produced from ORIGEN simulations for four different uranium signatures from gaseous centrifuge and gaseous diffusion enriched uranium, both with and without  $^{236}\text{U}$  present in the original material. The results from the inverse model were consistently higher than the exact values for the original material attributes. The resulting error may be attributed to the assumption made when developing the algorithm that the atomic density of  $^{238}\text{U}$  did not change with time. Error propagations were done by hand to predict uncertainties in the attributes as well as to determine the sensitivity of these results to errors in the input data.

#### **Sensitivity of initial guess for $^{235}\text{U}$ concentration**

The algorithm was insensitive to the initial guess for  $^{235}\text{U}$  concentration. In all cases less than 10 iterations (less than 1 second computational time) were used to acquire a result. The results presented in Table V verified that for any positive initial guess of any order of magnitude input into the algorithm will be iterated to a reasonably correct answer.

TABLE V.

Comparison of values calculated by the inverse model with various initial guesses for the  $^{235}\text{U}$  concentration to the actual values.

Enrichment Process	Initial Guess ( $N^{235}/N^{238}$ ) <sub>0</sub>	Original Value ( $N^{235}/N^{238}$ ) <sub>0</sub>	Inverse Model ( $N^{235}/N^{238}$ ) <sub>0</sub>	Percent Error
Centrifuge (with $^{236}\text{U}$ )	$1.00 \times 10^{10}$	42.4	$43.1 \pm 0.431$	1.61%
Diffusion (no $^{236}\text{U}$ )	$1.00 \times 10^{-10}$	22.4	$22.6 \pm 0.225$	0.66%

### Sensitivity of error in calculated $^{234}\text{U}$ attribute

Error propagations were done by hand to predict uncertainties in the attributes as well as to determine the sensitivity of the results to the input data. Beginning with the equation derived for the original  $^{234}\text{U}/^{238}\text{U}$  value, the error in the calculated  $^{234}\text{U}/^{238}\text{U}$  isotopic ratio was determined by first substituting the equation for the total number of fissions in the device into the equation for the original  $^{234}\text{U}/^{238}\text{U}$  value, resulting in the following equation for the  $^{234}\text{U}/^{238}\text{U}$  value:

$$\left(\frac{N^{234}}{N^{238}}\right)_0^i = \left(\frac{N^{232}}{N^{238}}\right)_T \left(\frac{N^{238}}{N^{89}}\right)_T \frac{Y^{89} \cdot M^{238}}{M^{235}} \frac{\sigma_f^{235}}{\sigma_{3n}^{234}} \left(\frac{N^{235}}{N^{238}}\right)_0^{i-1} \quad (4.1)$$

where substituting the equation for the total number of fissions in the device caused Avogadro's number ( $N_A$ ), the recoverable energy per fission ( $E_R$ ), and the  $^{235}\text{U}$  enrichment ( $e_0^{235}$ ) terms to cancel out. Then using error propagations the following equation was derived for the resulting error in the original  $^{234}\text{U}/^{238}\text{U}$  value:

$$\left( \frac{\epsilon N^{234}}{(N^{234})_0^i} \right)^2 = \left( \frac{M^{238}}{M^{235}} \right)^2 \left[ \left( \frac{\epsilon N^{232}}{N^{232}} \right)_T^2 + \left( \frac{\epsilon Y^{89}}{Y^{89}} \right)^2 + \left( \frac{\epsilon N^{89}}{N^{89}} \right)^2 + \left( \frac{\epsilon \sigma_f^{235}}{\sigma_f^{235}} \right)^2 + \left( \frac{\epsilon \sigma_{3n}^{234}}{\sigma_{3n}^{234}} \right)^2 + \left( \frac{\epsilon N^{235}}{(N^{235})_0^{i-1}} \right)^2 \right] \quad (4.2)$$

In order to determine the sensitivity of the error in the  $^{234}\text{U}/^{238}\text{U}$  value, Eq. (4.2) was used to plot the error in the calculated  $^{234}\text{U}/^{238}\text{U}$  value as a function of the error in the measured  $^{232}\text{U}$  value and the  $^{234}\text{U}(n, 3n)$  microscopic cross-section. The plot depicted in Fig. 8 shows that the calculated error in the  $^{234}\text{U}/^{238}\text{U}$  value varies linearly as a function of the error in the measured  $^{232}\text{U}$  value and the error in the  $^{234}\text{U}(n, 3n)$  microscopic cross-section. The linear relationship determined is important because it indicates that error in the measured  $^{232}\text{U}$  value and the error in the  $^{234}\text{U}(n, 3n)$  microscopic cross-section equally contribute to overall error in the calculated the  $^{234}\text{U}/^{238}\text{U}$  value. This relationship may also be utilized to determine the point at which reducing these errors no longer reduces the overall error in the calculated the  $^{234}\text{U}/^{238}\text{U}$  value.



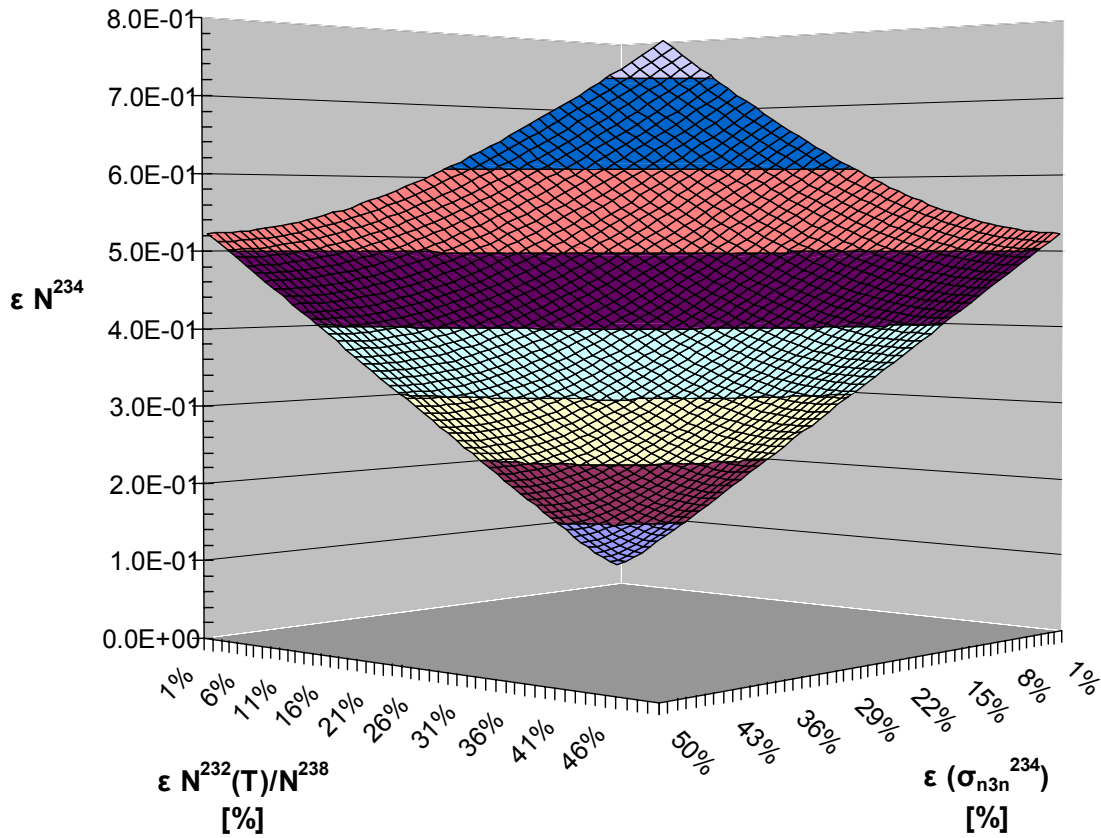


Fig. 8. Error in the calculated  $^{234}\text{U}/^{238}\text{U}$  value as a function of the error in the measured  $^{232}\text{U}$  value and the  $^{234}\text{U}(n, 3n)$  microscopic cross-section.

### Sensitivity of error in calculated $^{235}\text{U}$ attribute

Similar to the derivation for the error in the calculated  $^{234}\text{U}/^{238}\text{U}$  isotopic ratio, the error in the calculated  $^{235}\text{U}/^{238}\text{U}$  isotopic ratio was derived by first substituting the equation for the total number of fissions in the device into the equation for the original  $^{235}\text{U}/^{238}\text{U}$  value resulting in following equation for the  $^{235}\text{U}/^{238}\text{U}$  value:

$$\left(\frac{N^{235}}{N^{238}}\right)_0^i = \left(\frac{N^{235}}{N^{238}}\right)_T + \left(\frac{N^{89}}{N^{238}}\right)_T \frac{M^{235}}{M^{238}} Y^{89} \cdot \frac{\sigma_a^{235}}{\sigma_f^{235}} \cdot (e_0^i)^2 \quad (4.3)$$

where substituting the equation for the total number of fissions in the device caused Avogadro's number ( $N_A$ ) and the recoverable energy per fission ( $E_R$ ) terms to cancel out, and squared the term for the  $^{235}\text{U}$  enrichment ( $e_0^{235}$ ). The error in the original  $^{235}\text{U}/^{238}\text{U}$  value was derived by separating Eq. (4.3) into parts A and B in order to facilitate the error propagations. The following equations represent the equations for A and B and the resulting error in the calculated  $^{235}\text{U}/^{238}\text{U}$  value:

$$A = \left( \frac{N^{89}}{N^{238}} \right)_T \frac{M^{235}}{M^{238}} Y^{89} \cdot \frac{\sigma_a^{235}}{\sigma_f^{235}} \cdot (e_0^i)^2 \quad (4.4)$$

$$\varepsilon_A^2 = A^2 \cdot \left( \frac{M^{235}}{M^{238}} \right)^2 \left[ \left( \frac{\varepsilon Y^{89}}{Y^{89}} \right)^2 + \left( \frac{\varepsilon N^{89}}{N^{89}} \right)^2 + \left( \frac{\varepsilon \sigma_f^{235}}{\sigma_f^{235}} \right)^2 + \left( \frac{\varepsilon \sigma_a^{235}}{\sigma_a^{235}} \right)^2 + \left( \frac{\varepsilon e_0^i}{e_0^i} \right)^4 \right] \quad (4.5)$$

$$B = \left( \frac{N^{235}}{N^{238}} \right)_0^i = \left( \frac{N^{235}}{N^{238}} \right)_T + A \quad (4.6)$$

$$\varepsilon_B^2 = \varepsilon^2 (N^{235})_T + \varepsilon_A^2 \quad (4.7)$$

The sensitivity of the error in the  $^{235}\text{U}/^{238}\text{U}$  value was determined by plotting the error in the calculated  $^{235}\text{U}/^{238}\text{U}$  value as a function of the error in the  $^{235}\text{U}$  enrichment and the error in the  $^{235}\text{U}$  microscopic fission cross-section. The plot depicted in Fig. 9 shows that the calculated error in the  $^{235}\text{U}/^{238}\text{U}$  value varies linearly as a function of the error in the  $^{235}\text{U}$  microscopic fission cross-section and varies nonlinearly as a function of the

error in the  $^{235}\text{U}$  enrichment. The nonlinear relationship determined indicates that error in the  $^{235}\text{U}$  enrichment contributes more towards the overall error in the calculated the  $^{235}\text{U}/^{238}\text{U}$  value than the error in the  $^{235}\text{U}$  microscopic fission cross-section does. Therefore, more effort should be spent reducing the error in the value for the  $^{235}\text{U}$  enrichment than reducing the error in the  $^{235}\text{U}$  microscopic fission cross-section.

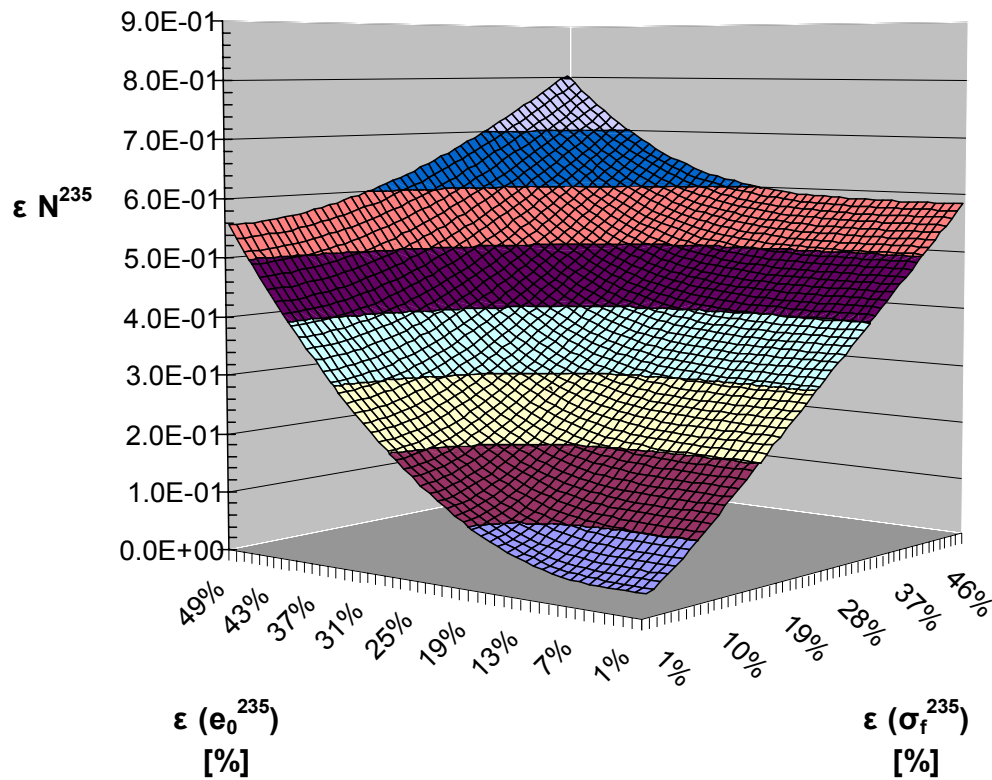


Fig. 9. Error in the calculated  $^{235}\text{U}/^{238}\text{U}$  value as a function of the error in the  $^{235}\text{U}$  enrichment and the  $^{235}\text{U}$  microscopic fission cross-section.

**Sensitivity of error in calculated  $^{236}\text{U}$  attribute**

The derivation for the error in the calculated  $^{236}\text{U}/^{238}\text{U}$  isotopic ratio is provided in Appendix B. The sensitivity of the error in the  $^{236}\text{U}/^{238}\text{U}$  value was determined by plotting the error in the calculated  $^{236}\text{U}/^{238}\text{U}$  value as a function of the errors in the  $^{236}\text{U}$  and the  $^{235}\text{U}$  microscopic absorption cross-sections. The plot depicted in Fig. 10 shows that the calculated error in the  $^{236}\text{U}/^{238}\text{U}$  value varies linearly as a function of the errors in the  $^{236}\text{U}$  and the  $^{235}\text{U}$  microscopic absorption cross-sections. The linear relationship determined indicates that the error in the  $^{235}\text{U}$  microscopic absorption cross-section affects the overall error in the calculated the  $^{236}\text{U}/^{238}\text{U}$  value more than the error in the  $^{236}\text{U}$  microscopic absorption cross-section. This is because increasing the error in the  $^{235}\text{U}$  microscopic absorption cross-section increases the overall error in the calculated the  $^{236}\text{U}/^{238}\text{U}$  value significantly more than increasing the error in the  $^{236}\text{U}$  microscopic absorption cross-section does. Therefore, more effort should be spent reducing the error in the  $^{235}\text{U}$  microscopic absorption cross-section than reducing the error in the  $^{236}\text{U}$  microscopic absorption cross-section.

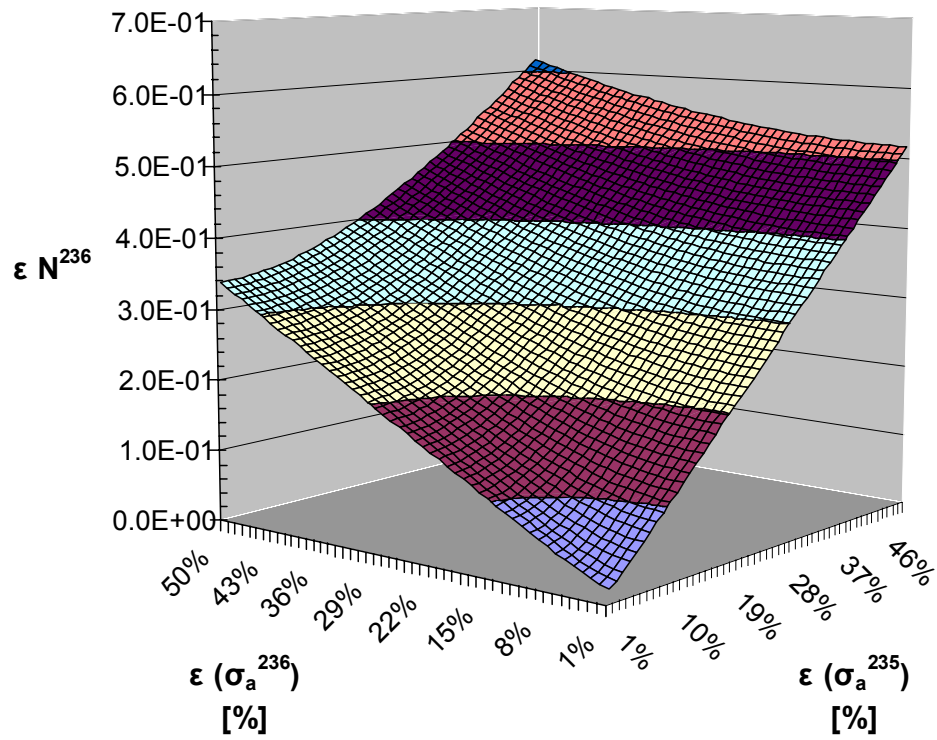


Fig. 10. Error in the calculated  $^{236}\text{U}/^{238}\text{U}$  value as a function of the errors in the  $^{236}\text{U}$  and the  $^{235}\text{U}$  microscopic absorption cross-sections.

## CHAPTER V

### $^{234}\text{U}$ ISOTOPICS IN MINES

Different uranium mines throughout the world are characterized by different isotopic abundances of  $^{234}\text{U}$  which may be used as a signature to indicate the geographic origin of the material.  $^{234}\text{U}$  has a relatively short half-life and exists in secular equilibrium with  $^{238}\text{U}$ . Thus, the ratio of  $^{234}\text{U}$  to  $^{238}\text{U}$  should equal to the ratio of the half-lives (53.8 ppm). Variations in the ratio of  $^{234}\text{U}/^{238}\text{U}$  may result from processes that disrupt the decay chain of  $^{238}\text{U}$  to  $^{234}\text{U}$ .<sup>7</sup> All of the measured  $^{234}\text{U}/^{238}\text{U}$  values shown in Table VI were measured directly using thermal ionization mass spectrometry where the  $^{235}\text{U}^+$  ion beam intensity was adjusted to correct for mass discrimination using the measured  $^{235}\text{U}/^{238}\text{U}$  ratio obtained by gas source mass spectrometry.<sup>7, 14</sup>

TABLE VI.

Variations in measured  $^{234}\text{U}/^{238}\text{U}$  atom ratios from mines throughout the world.<sup>7,14</sup>

Sample No.	Country of Origin	Milling Facility	$^{234}\text{U}/^{238}\text{U}$ Atom Ratio	Statistical Uncertainty
1	Finland	Askola	5.444E-05	8.0E-08
2	Finland	Paukkajanvaara	5.126E-05	7.6E-07
3	Australia	Ranger Mine	5.455E-05	4.4E-07
4	Australia	Dam Operations	5.341E-05	6.2E-07
5	Canada	Cogema Resources	5.385E-05	6.0E-07
6	Canada	CAMECO Key Lake Op.	5.397E-05	3.4E-07
7	Gabon	Comuf Mounana	5.434E-05	4.2E-07
8	Czech Republic	DIAMO, Straz pod Ralskem	8.355E-05	4.9E-07
9	Canada	CAMECO Rabbit Lake Op.	5.444E-05	4.8E-07
10	Namibia	Roessing Uranium Mine	5.460E-05	4.1E-07
11	France	Cogema Lodeve	5.154E-05	2.8E-07
12	France	CETAMA Amethyste	5.340E-05	3.3E-07

A plot of the measured  $^{234}\text{U}/^{238}\text{U}$  atom ratios with associated uncertainties for all twelve samples is depicted in Fig. 11. Sample 8 from the Czech Republic has a significantly greater  $^{234}\text{U}/^{238}\text{U}$  atom ratio than any other sample which cannot be explained by geological processes. One possibility may be a result of anthropogenic contamination with plutonium, especially  $^{238}\text{Pu}$ .<sup>7</sup> This contamination may have occurred as a result of the Chernobyl accident. A more in depth comparison of the variation in the measured  $^{234}\text{U}/^{238}\text{U}$  atom ratios with associated uncertainties with sample 8 omitted is depicted in Fig. 12.

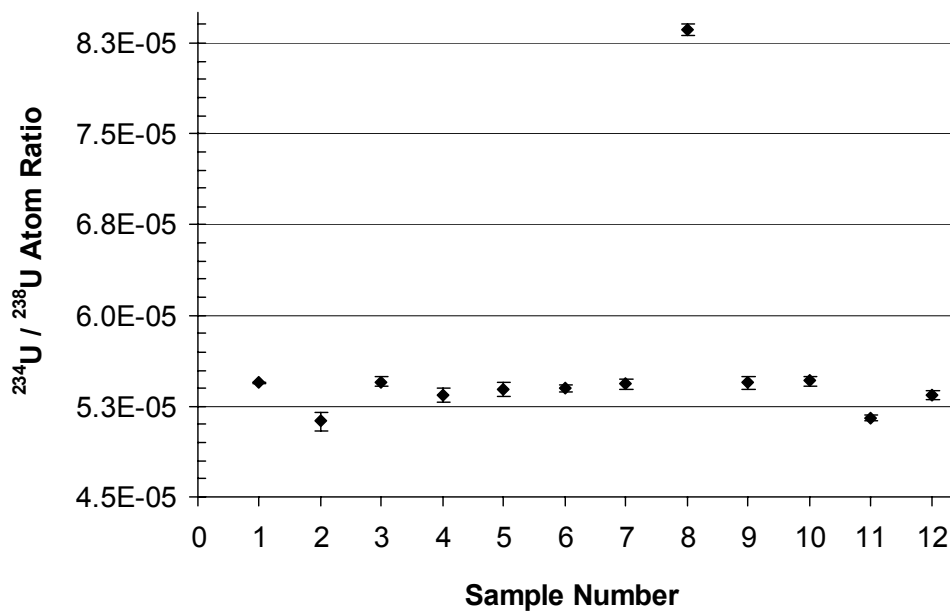


Fig. 11. The  $^{234}\text{U}/^{238}\text{U}$  atom ratio measured in all twelve samples.<sup>7, 14</sup>

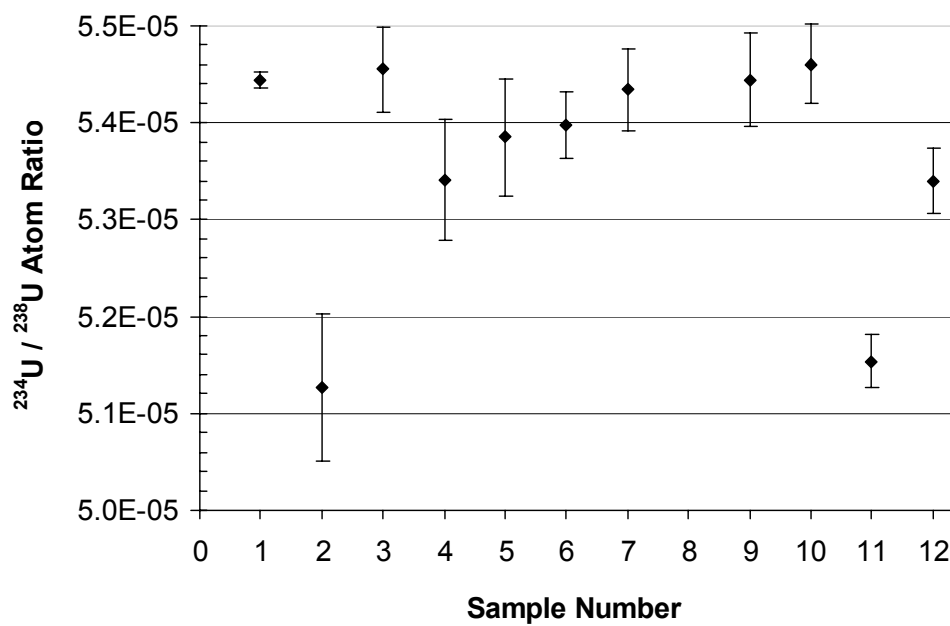


Fig. 12. Expanded plot of the measured  $^{234}\text{U}/^{238}\text{U}$  atom ratios excluding sample 8.<sup>7, 14</sup>



## CHAPTER VI

### DISCUSSION AND CONCLUSION

#### **Discussion**

Various methods that could potentially be used to disguise the origin of the nuclear material used in HEU weapon prior to it being detonated were assessed in order to determine their effects on the validity of the algorithm. The first spoofing technique assessed was contamination of the original material used in the HEU weapon with fission products such as  $^{137}\text{Cs}$  or  $^{60}\text{Co}$ . This will result in higher measured post-detonation concentrations of the fission products used to contaminate the original weapons material. The total number of fissions in the device per unit mass will be affected if the fission products used to contaminate the original material are the same as the fission products used in this calculation. Using two fission products significantly increases the probability of determining that original material was contaminated because there is a smaller probability that the two fission products used in the algorithm were also used to contaminate the original material. If only one of the fission products that was used in the algorithm was also used to contaminate the original material, then the total number of fissions in the device calculated using one fission product will differ significantly from the value calculated using the other fission product. Thus, indicating that one of the fission products was either present in the original material or else measured incorrectly.

The second spoofing technique assessed was surrounding a metal uranium sphere with higher actinides such as  $^{241}\text{Am}$  or  $^{237}\text{Np}$ . This presents a considerably more difficult problem because all of the measured post-detonation fission product concentrations will be higher. Therefore, it is harder to determine obvious outliers from fission product concentrations that would indicate the original material was contaminated prior to being detonated. In this case, the contamination of the original material with higher actinides may be determined by measuring the concentrations of several higher actinides to see if any stand out as being much larger than the rest.

Another spoofing technique assessed was boosting the weapon prior to detonation. In a boosted nuclear weapon, a mixture of deuterium (D) and tritium (T) gas is injected into the central core of  $^{235}\text{U}$  metal sphere, called the “pit”. The implosion of the pit causes the  $^{235}\text{U}$  to fission which in turn causes the atoms in the D-T mixture to undergo fusion. The fusion reaction produces large quantities of high energy neutrons (approximately 14 MeV) which travel through the compressed pit causing additional fission reactions.<sup>11</sup> The boosting of a nuclear weapon greatly increases the yield by causing more of the material to fission during detonation. Therefore, if calculated yield of an HEU weapon was on the order of 100 kT or greater it was probably boosted. In the case where a weapon was boosted prior to being detonated but was a fizzle, then the atoms in the D-T mixture did not undergo fusion and post-detonation measurements of both deuterium and tritium could be obtained.

The last spoofing technique assessed was using a combination of plutonium and uranium metal or Mixed Oxide fuel (MOX) fuel as the original material in the weapon. This presents the most difficult problem because not only will the concentrations of the fission product be higher but any signatures indicating the method of enrichment will disappear. In this case, it might be useful to combine techniques used to determine the original material in both an HEU and plutonium device.

### **Conclusion**

In this work, an algorithm was developed that uses measured isotopic ratios from fission products and actinides present following the detonation of a nuclear weapon to compute the original material attributes of the weapon. The algorithm was comprised of analytical inversions of first-order differential equations derived directly from burnup and radioactive decay equations. The following post-detonation isotopic ratios were used:  $^{89}\text{Sr}/^{238}\text{U}$ ,  $^{95}\text{Zr}/^{238}\text{U}$ ,  $^{232}\text{U}/^{238}\text{U}$ ,  $^{234}\text{U}/^{238}\text{U}$ ,  $^{235}\text{U}/^{238}\text{U}$ , and  $^{236}\text{U}/^{238}\text{U}$ . The primary advantage gained from this methodology was it provided accurate solutions with essentially no computational time required. Error propagations were used to determine the sensitivity of the error in the calculated original  $^{234}\text{U}$ ,  $^{235}\text{U}$ , and  $^{236}\text{U}$  attributes for the HEU fuel. The errors in the calculated  $^{234}\text{U}/^{238}\text{U}$  and  $^{236}\text{U}/^{238}\text{U}$  attributes were linearly related to the errors in measured parameters. The error in the calculated  $^{235}\text{U}/^{238}\text{U}$  attribute varied nonlinearly as a function of the  $^{235}\text{U}$  enrichment placing a significant importance on ensuring the accuracy of this value. The determined signature that indicated the enrichment process used to create the weapons material was based on the calculated

$^{234}\text{U}/^{238}\text{U}$  ratio in the inverse model. A source of error that was not assessed exists in the cross-section data used throughout the algorithm from the ORIGEN2 library for an FFTFC reactor. In this work, we were only testing the feasibility of the algorithm and did not consider its relationship to an actual weapon detonation. Thus, testing of this methodology using cross-section data obtained for an actual device detonation would improve the viability of the algorithm.

This work is important to homeland security and a significant prototype to data protocol in the event of a terrorist attack in our country. The algorithm developed was restricted only to HEU devices; however, future efforts will consider plutonium devices as well. It is also necessary to analyze how elements disperse in the environment and what current technology is available to measure isotopic fission fragments in the environment. All of the above aspects will affect the validity of the algorithm and if it could in fact be used if a terrorist device was detonated in the U.S.

## REFERENCES

1. R.F. MOZLEY, *The Politics and Technology of Nuclear Proliferation*, University of Washington Press, Seattle (1984).
2. “Table of Nuclides,” Korea Atomic Energy Research Institute Website, available on the Internet at <<http://atom.kaeri.re.kr/ton/>>
3. K.J. MOODY, *Nuclear Forensics Analysis*, Taylor and Francis Group, New York, (2005).
4. “Identifying the Source of Stolen Nuclear Materials,” Lawrence Livermore National Laboratory, Science and Technology Review, January/February 2007.
5. A.M. LAFLEUR and W.S. CHARLTON, “A Method for Determining Material Attributes from Post-Detonation Fission Product Measurements of an HEU Device,” *Proc. of the 46th Annual Meeting of the Institute for Nuclear Materials Management*, Nashville, Tennessee, July 16-20, 2006.
6. M.R. SCOTT, “Nuclear Forensics: Attributing the source of Spent Fuel Used in an RDD Event,” M.S. Thesis, Texas A&M University, 2005.
7. S. RICHTER, A. ALONSO, W. DE BOLLE, R. WELLUM, and P.D.P. TAYLOR, ‘Isotopic “fingerprints” for Natural Uranium Ore Samples,’ *Int J Mass Spectrom*, **193**, 19 (1999).
8. A.G. CROFF, “A User’s Manual for the ORIGEN2 Computer Code,” ORNL/TM7175, Oak Ridge National Laboratory (1980).

9. “Uranium Enrichment,” Urenco Website, available on the Internet at <http://www.urenco.de>
10. “Fact Sheet on Uranium Enrichment,” U.S. Nuclear Regulatory Commission Website, available on the Internet at <http://www.nrc.gov/reading-rm/doc-collections/fact-sheets/enrichment.html>
11. “Appendix B: The Eight Major Processes of the Nuclear Weapons Complex,” U.S. Department of Energy Website, available on the Internet at [www.lm.doe.gov/documents/3\\_pro\\_doc/lts\\_study/legacy\\_story/117\\_206.pdf](http://www.lm.doe.gov/documents/3_pro_doc/lts_study/legacy_story/117_206.pdf).
12. “Chapter 3.28 Systems, Equipment and Components for Use in Laser Based Enrichment Plants,” available on the Internet at <http://www.iraqwatch.org/government/US/DOE/DOE-CHAPTER3.PDF>
13. M. BENEDICT, T. PIGFORD, and H. LEVI, *Nuclear Chemical Engineering*, McGraw-Hill, New York, (1981).
14. R. OVASKAINEN, K. MAYER, W. DE BOLLE, D. DONOHUE, and P. DE BIEVRE, *Proc. of the 19th Annual Symposium on Safeguards and Nuclear Material Management*, Montpellier, May 13–15, 1997, C. Foggi, F. Genoni (Eds.) Ispra, ESARDA No. 28.

## **APPENDIX A**

### **AN EXAMPLE OF ORIGEN2 DECK**

Below is an example of the ORIGEN2 deck used to simulate the detonation of an HEU weapon.

```

-1
-1
-1
RDA Irradiation of 1 MT of fuel
RDA Fuel enrichment is 95.0 w/o U-235
RDA
LIB 0 1 2 3 381 382 383 9 50 0 1 0
INP 1 1 -1 -1 1 1
BUP
IRP 0.0250 387037.0 1 2 4 2 BURNUP=9676 MWD/MT
IRP 0.0500 387037.0 2 3 4 0 BURNUP=19352 MWD/MT
IRP 0.1000 387037.0 3 4 4 0 BURNUP=38704 MWD/MT
DEC 1.1000 4 5 4 0 DECAY FOR 1.100 DAYS
BUP
OPTL 8 8 8 8 8 8 8 8 8 8 8 7*8 5*8 8
OPTA 8 8 8 8 2 8 7 8 7 8 8 7*8 5*8 8
OPTF 8 8 8 8 7 8 7 8 7 8 8 7*8 5*8 8
OUT 5 1 -1 0
END
2 922340 7600. 922350 950000. 922380 42400. 0 0.0
0

```



**APPENDIX B****CALCULATION OF ERROR IN  $^{236}\text{U}/^{238}\text{U}$  ATTRIBUTE**

The derivation for the error in the calculated  $^{236}\text{U}/^{238}\text{U}$  attribute is long. The following equation for the  $^{236}\text{U}/^{238}\text{U}$  isotopic ratio was obtained by substituting the equation for the total number of fissions in the device into the equation derived for the original  $^{236}\text{U}/^{238}\text{U}$  value:

$$\left(\frac{N^{236}}{N^{238}}\right)_0^i = \left(\frac{N^{236}}{N^{238}}\right)_T - \left(\frac{N^{235}}{N^{238}}\right)_0^i \left(\frac{N^{238}}{N^{235}}\right)_0^{i-1} \left(\frac{N^{89}}{N^{238}}\right)_T \frac{M^{235}}{M^{238}} \frac{1}{Y^{89} \cdot \sigma_f^{235}} \left\{ \sigma_a^{235} - \sigma_f^{235} - \frac{\sigma_a^{236}}{2} \left[ \left(\frac{N^{236}}{N^{235}}\right)_T + \left(\frac{N^{236}}{N^{235}}\right)_0^{i-1} \right] \right\} \quad (\text{B.1})$$

Several sub-variables are defined to avoid having the equations stretch out across multiple pages and to facilitate the error propagations. The sub-variables are used to simplify the solution and are not related to any physical concepts. The error in a given equation is represented by  $\varepsilon$ . The sub-variables A - F are defined as:

$$A = \left[ \left(\frac{N^{236}}{N^{235}}\right)_T + \left(\frac{N^{236}}{N^{235}}\right)_0^{i-1} \right] \quad (\text{B.2})$$

$$\begin{aligned} \varepsilon_A^2 = & \left\{ \left[ \frac{\varepsilon(N^{236})_T}{(N^{236})_T} \right]^2 + \left[ \frac{\varepsilon(N^{235})_T}{(N^{235})_T} \right]^2 \right\} \cdot \left[ \left( \frac{N^{236}}{N^{235}} \right)_T \right]^2 \\ & + \left\{ \left[ \frac{\varepsilon(N^{236})_0^{i-1}}{(N^{236})_0^{i-1}} \right]^2 + \left[ \frac{\varepsilon(N^{235})_0^i}{(N^{235})_0^i} \right]^2 \right\} \cdot \left[ \left( \frac{N^{236}}{N^{235}} \right)_0^{i-1} \right]^2 \end{aligned} \quad (\text{B.3})$$

$$B = \frac{1}{2} \sigma_a^{236} A \quad (\text{B.4})$$

$$\varepsilon_B^2 = \frac{1}{4} B^2 \cdot \left[ \left( \frac{\varepsilon \sigma_a^{236}}{\sigma_a^{236}} \right)^2 + \left( \frac{\varepsilon_A}{A} \right)^2 \right] \quad (\text{B.5})$$

$$C = \sigma_a^{235} - \sigma_f^{235} - B \quad (\text{B.6})$$

$$\varepsilon_C^2 = \varepsilon^2 (\sigma_a^{235}) + \varepsilon^2 (\sigma_f^{235}) + \varepsilon_B^2 \quad (\text{B.7})$$

$$D = \left( \frac{N^{235}}{N^{238}} \right)_0^i \left( \frac{N^{238}}{N^{235}} \right)_0^{i-1} \left( \frac{N^{89}}{N^{238}} \right)_T \frac{1}{Y^{89} \cdot \sigma_f^{235}} \cdot C \quad (\text{B.8})$$

$$\varepsilon_D^2 = D^2 \cdot \left\{ \frac{\left[ \frac{\varepsilon \left( \frac{N^{235}}{N^{238}} \right)_0^i}{\left( \frac{N^{235}}{N^{238}} \right)_0^i} \right]}{\left[ \frac{\varepsilon \left( \frac{N^{238}}{N^{235}} \right)_0^{i-1}}{\left( \frac{N^{238}}{N^{235}} \right)_0^{i-1}} \right]} + \left[ \frac{\varepsilon Y^{89}}{Y^{89}} \right]^2 + \left[ \frac{\varepsilon N^{89}}{N^{89}} \right]^2 + \left[ \frac{\varepsilon \sigma_f^{235}}{\sigma_f^{235}} \right]^2 + \left[ \frac{\varepsilon_C}{C} \right]^2 \right\} \quad (\text{B.9})$$

$$E = D \frac{M^{235}}{M^{238}} \quad (\text{B.10})$$

$$\mathcal{E}_E^2 = \mathcal{E}_D^2 \left( \frac{M^{235}}{M^{238}} \right)^2 \quad (\text{B.11})$$

$$F = \left( \frac{N^{236}}{N^{238}} \right)_0^i = \left( \frac{N^{236}}{N^{238}} \right)_T - E \quad (\text{B.12})$$

$$\mathcal{E}_F^2 = \mathcal{E}^2 (N^{236})_T + \mathcal{E}_E^2 \quad (\text{B.13})$$

## CONTACT INFORMATION

Name: Adrienne Marie LaFleur

Professional Address: c/o Dr. William Charlton  
Department of Nuclear Engineering  
Texas A&M University  
College Station, TX 77843-3133

Email Address: [amlafleur@tamu.edu](mailto:amlafleur@tamu.edu)

Education: BS Nuclear Engineering, Minor in Mathematics  
Texas A&M University, May 2007  
Undergraduate Research Scholar